[1.]F. C. NJOKU, [2.]O. IKANI, [3.]A.A. OKPEH, [4.]R. JERRY, [5.]A.O. ADIKPE, [6.]S. N. OBIAHU

MOBILITY–AWARE HANDOVER SCHEME FOR MILLIMETERWAVE HETNET: A CARTESIAN–PLANE APPROACH

[1,4] Telecommunications Engineering Department, Faculty of Ground Engineering, Air Force Institute of Technology, Kaduna, NIGERIA
[2] Information and Communications Technology Department, Faculty of Ground Engineering, Air Force Institute of Technology, Kaduna, NIGERIA
[3,5] Electronics and Telecommunications Engineering Department, Faculty of Engineering, Ahmadu Bello University, Zaria, Kaduna, NIGERIA
[6] Computer Engineering Department, Faculty of Engineering, Ahmadu Bello University, Zaria, Kaduna, NIGERIA

Abstract: This paper proposes a mobility–aware handover scheme for millimeter–Wave (mmWave) heterogeneous networks (HetNets) based on a Cartesian–plane approach (CPH). The scheme leverages the unique characteristics of mmWave propagation, spatial distribution, mobility pattern of User equipment (UE) and the available bandwidth in each cell to select the most suitable cell to achieve seamless handover and enhance network performance. The CPH scheme utilizes a Cartesian coordinate system for UE position estimation and prediction. This approach allows for efficient calculation of the distance between UEs and available base stations (BSs), enabling rapid handover decision making. It also incorporates the concepts of obstacle–free and obstacle–based coefficients in relation to Line–of–Sight (LoS) and Non–Line–of–Sight (NLoS) communication links. The technique is evaluated through simulations, demonstrating its effectiveness in improving handover success rate, and enhancing network throughput compared to the standard Rate–based handover (RBH) and the Seamless Handover Technique (SMART) handover models using number of handovers and average throughput as performance metrics. Simulation results obtained showed that the proposed scheme in terms of number of Femto Base Station (FBS) achieved 53.98% and 6.87% handover percentage reduction and 9.39% and 9.15% average throughput percentage improvement respectively when compared to the existing handover models.
Keywords: Handover, LoS, NLoS, Obstacle–free coefficient, Obstacle–based coefficient, UE

1. INTRODUCTION

Millimeter–Wave (mmWave) technology has gained significant attention in recent years due to the increasing demand for high–data–rate applications [1]. The frequency bands used in mmWave technology range from 24 GHz to 100 GHz, offering vast bandwidths and high data rates. However, mmWave signals have a shorter range and are more susceptible to blockages compared to lower–frequency signals [2]. Heterogeneous networks (HetNet) consist of multiple tiers of networks with different transmit powers and cell sizes. In the context of mmWave HetNet, macro cells operating at lower frequencies are overlaid with small cells operating at higher frequencies, resulting in increased network capacity and coverage [21][26][27]. Massive deployment of small cells is seen to be a vital innovation in 5G, which enables frequent frequency reuse and higher data rates [21]. Small cells, however, present a major challenge for users moving at high speeds [12]. This is because the smaller coverage areas of small cells lead to frequent handover, resulting in lower throughput and longer delay [18]. Furthermore, 5G networks are characterized by extensive bandwidth at millimetreWave (mmWave) frequencies to offer high data rate services in cellular networks [11]. Although mmWave signals can provide extensive bandwidth, they are more sensitive to blockage effects than conventional lower band signals [20]. Therefore, mmWave bands experience severe received signals attenuation due to blockages caused by buildings, trees, and even the user's hand or body [13]. Overcoming the channel quality gap between Line–of–Sight (LoS) to Non–LoS (NLoS) conditions in mmWave bands still poses a major challenge in 5G networks since it can reduce the network capacity and user Quality–of–Experience (QoE) [19]. One such innovative approach is the Cartesian–plane handover scheme, which focuses on enhancing positional modeling for UE within the network. By leveraging Cartesian coordinates, this scheme aims to improve the accuracy and reliability of UE positioning, thereby facilitating smoother handovers between different network nodes in MillimeterWave HetNets. By introducing the concepts of

ISSN 1584 – 2665 (printed version); ISSN 2601 – 2332 (online); ISSN-L 1584 – 2665

obstacle–free and obstacle–based coefficients based on Cartesian coordinates, this scheme aims to optimize handover decisions, improve average system throughput, and ensure uninterrupted connectivity for users moving across different network cells within a millimeter–wave heterogeneous environment.

2. KEY CONTRIBUTIONS

The adoption of a Cartesian–plane handover scheme enhances mobility support for UEs moving within MillimeterWave HetNets. With accurate positional modeling, seamless handovers can be executed as UEs transition between different cells or access points, ensuring uninterrupted connectivity and minimal service disruptions. The unresolved problem of when and where to handover arising from signal blockages as well as the user changing direction still poses a great challenge for LoS and NLoS communication link users in mmWave heterogeneous network. Hence this paper presents a Cartesian–plane handover scheme for seamless communication in MillimeterWave heterogeneous network. By modeling the user movement pattern as obstacle–free and obstacle–based coefficients in relation to LoS and NLoS communication links, this proposed scheme guarantees better performance in terms of reducing the number of handovers and boosting the average throughput thus improving on the overall Quality of Experience (QoE) and Quality of Service (QoS) of the users most of which were not achieved by previous researchers.

3. LITERATURE REVIEW

[16] presented a SMART handoff policy for mmWave HetNets based on reinforcement learning. In SMART, the handoff trigger conditions were derived by taking into accounts both mm–Wave channel characteristics and QoS requirements of UEs. [4] analyzed a velocity–aware handover management scheme for two–tier downlink cellular network to mitigate the handover effect on the foreseen densification throughput gains. [6] proposed a cell selection scheme for handover reduction based on movement direction and velocity of UEs for 5G multi–layered radio access networks (RANs) architecture. [17] developed a novel 5G wireless network architecture that comprised of two main aspects of massive MIMO–OFDMA and IP based vertical handover. The proposed architecture divided the whole macro area network into microcells and each micro–cell consisted of multiple small cells. [9] presented an optimal Evolved NodeB (eNB) selection mechanism for 5G intra–mobility HO based on spatial information of the sparse eNB network. The authors proposed two different networks based on eNB density: Sparse and dense. [25] also applied the idea of fuzzy logic and used user speed and wireless channel quality parameters to adjust the hysteresis threshold of the handover strategy in a self–optimizing way, so as to reduce the number of redundant handovers and the probability of handover failure. The proposed algorithm in [15] estimated handover parameter settings based on the weight function, which depends on three bounded functions and the weight of each bounded function. In [7], a handover–based image–to–decision is proposed with Deep Q–learning, which can map pictures to a handover decision of UE. [10] proposed an offline strategy based on double deep reinforcement learning (DDRL) to reduce the frequency of handovers (HOs) in millimeter–wave networks, therefore lowering the users' poor quality of service. [22] proposed an adaptive joint handover decision algorithm which was realized via a genetic algorithm. Based on the genetic algorithm, the dynamic hysteresis margin that met the requirement of fast handover at different moving speeds was achieved by optimizing the handover parameters, thus achieving a higher probability of communication satisfaction. [3] proposed a robust algorithm to analyze the relationship between hysteresis margin and trigger time through a novel mechanism that dynamically set the control parameters of handover in order to reduce unnecessary handover thereby ushering innovative ideas for the research of handover in HetNets. [5] proposed an adaptive adjustment algorithm for handover parameters based on fuzzy logic control. [14] proposed a dynamic obstacle tracking technique that is based on short–term historical link failure information. In the work, the authors

ISSN 1584 – 2665 (printed version); ISSN 2601 – 2332 (online); ISSN-L 1584 – 2665

made attempts at tracking multiple dynamic obstacles in a mm–Wave enabled coverage area in readiness for handover procedure.

4. METHODOLOGY: CONCEPTUAL SYSTEM NETWORK ARCHITECTURE

The conceptual network architecture is presented in Figure 1.

The equations that conceptually govern the UE LoS and NLoS communication links are expressed respectively as:

$$\mathrm{LoS}_{\text{communication link}} = \mathrm{d_l} \tag{1}$$

where, $\mathrm{d_l} < \mathrm{D_{max}}$

$$\mathrm{NLoS}_{\text{communication link}} = \mathrm{d_n} \tag{2}$$

where, $\mathrm{D_{max}} \leq \mathrm{d_n} < \mathrm{D_{FP}}$

The system architecture is a two–cell network. The base stations are randomly distributed in a Poisson point process, which is to maintain tractability of the user movement in both LoS and NLoS scenarios. User Equipment with the thick line circle ($\mathrm{d_l} < \mathrm{D_{max}}$) are assumed to have a LoS communication link while UE with ($\mathrm{D_{max}} \leq \mathrm{d_n} < \mathrm{D_{FP}}$) are assumed to be in an NLoS communication with the base station. Furthermore, in this conceptualized model, it is assumed that whenever the UE encounters an obstacle in its path (such as trees or buildings which serves as blockages to quality signal reception), its mobility pattern is modeled with respect to an obstacle–based coefficient. However, when the UE encounters no obstacle, its movement pattern is modeled with respect to an obstacle–free coefficient, hence its communication link is said to be LoS. Also, a UE is said to be a LoS communication link when its movement from a given point to other falls within the threshold distance of 200m [23] irrespective of the random mobility pattern of the UE. Additionally, the UE moves at varying speeds within both communication links. This conceptualized model is guaranteed to achieve better efficiency in appropriately selecting the best base station from the available densely deployed cells, hence minimizing both the number of handover and average running time as the UE moves in both LoS and NLoS communication links.

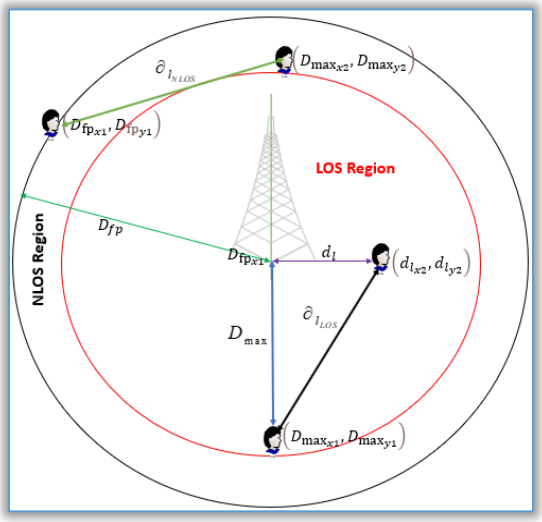

Figure 1: Conceptual System Architecture of the CBH–model

Figure 1 shows the LoS and NLoS system framework of the CBH –model. Where $\partial_{\mathrm{L_{los}}}$ stands for the distance between a UE that is D_max away from the base station and a UE that is in the LoS region. Also, $\partial_{\mathrm{L_{Nlos}}}$ represents the distance between UE at $\mathrm{D_{max}}$ LoS region and UE at $> \mathrm{D_{max}}$ transmission region.

Thus, the $\partial_{\mathrm{L_{los}}}$ distance [8] is given as:

$$\partial_{\mathrm{L_{los}}} = \sqrt{\left|(\mathrm{D_{max_{x1}}} - \mathrm{D_{max_{y1}}})^2\right| + \left|(\mathrm{d_{l_{x2}}} - \mathrm{d_{l_{y2}}})^2\right|} \tag{3}$$

$$\partial_{\mathrm{L_{los}}} = \sqrt{|(\mathrm{D_{max}})^2| + |(\mathrm{d_l})^2|} \tag{4}$$

Therefore, to obtain the UE distance whilst in LoS communication, Eq. (5) is presented:

$$\mathrm{d_o} = \sqrt{|(\mathrm{D_{max}})^2| + |(\mathrm{d_l})^2|} - \frac{1}{2}\mathrm{a}\vartheta^2 \tag{5}$$

By simplifying equation (5), the $\mathrm{d_o}$ can be re–written as equation (6):

$$\mathrm{d_o} = \partial_{\mathrm{L_{los}}} - \frac{1}{2}\mathrm{a}\vartheta^2 \tag{6}$$

where $\partial_{\mathrm{L_{los}}}$ is equal to $\sqrt{|(\mathrm{D_{max}})^2| + |(\mathrm{d_l})^2|}$ as given in Eq. (4)

Consequently, based on the $\mathrm{UE_i}$ placement, Eq. (6) is re–written in Eq. (7):

ISSN 1584 – 2665 (printed version); ISSN 2601 – 2332 (online); ISSN-L 1584 – 2665

$$d_o.UE_i = \partial_{L_{los}} UE_i - \frac{1}{2} a\vartheta^2.UE_i \quad (7)$$

Similarly, $\partial_{L_{nlos}}$ is assumed to be $(D_{max} \leq d_n < D_{fp})$. However, for the purpose of computational simplicity, this report assumed $\partial_{L_{nlos}}$ to be $(D_{max} < D_{fp})$.

Hence, $\partial_{L_{nlos}}$ distance is given as:

$$\partial_{L_{nlos}} = \sqrt{\left|(D_{FP_{x1}} - D_{max_{y1}})^2\right| + \left|(D_{FP_{x2}} - D_{FP_{y2}})^2\right|} \quad (8)$$

Thus, Eq. (8) can be defined as:

$$\sqrt{|(D_{FP})^2| + |(D_{max})^2|} = d_i + \frac{1}{2} a\vartheta^2 \quad (9)$$

Therefore, to compute the UE distance whilst in NLoS communication, Eq. (9) is re–arranged to give Eq. (10):

$$d_i = \sqrt{|(D_{FP})^2| + |(D_{max})^2|} - \frac{1}{2} a\vartheta^2 \quad (10)$$

Consequently, based on the UE_i placement, Eq. (10) is re–written in Eq. (11):

$$d_i.UE_i = \partial_{L_{nlos}} UE_i - \frac{1}{2} a\vartheta^2.UE_i \quad (11)$$

Hypothetical Coordinate for Movement of the UE

Conceptual representations of the obstacle–free and obstacle–based mobility patterns in respect to LoS and NLoS communication linkages, respectively, are shown in Figure 2 and Figure 3. The conceptual trajectory diagram, shown in Figure 1, shows the likely mobility pattern in relation to the location of the for LoS communication inside a Cartesian plane.

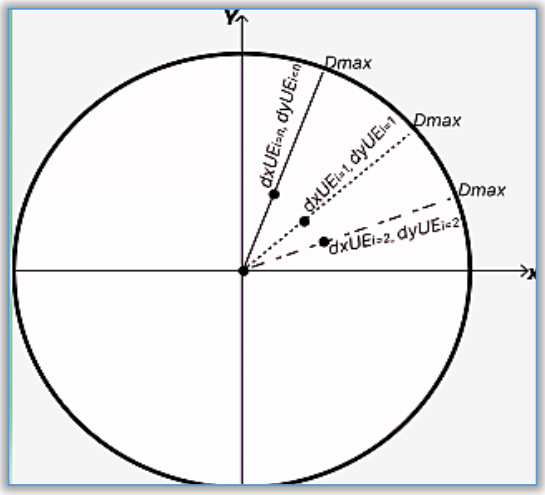

Figure 2: UE Placement Trajectory for Obstacle–free Scenario

This paper considered a typical density of the UEs in 5G to be around $300UEs/km^2$ [23]. A base station density range of $10 - 70\ BSs/km^2$ is used in this study. This range captures the 3GPP standard specifications for base station density with respect to the number of UEs/km^2 in ultra–dense networks [24]. Furthermore, Figure 2 defines the scenario whereby the $C_{x=0}$ exponent acts as an obstacle–free coefficient that shows the UE mobility pattern to be within a defined threshold, denoted as D_{max}. Therefore, so long as the UE movement remains within this set distance threshold, the UE is considered to be within LoS communication link with a base station. Additionally, it is assumed that a UE movement from an initial point to any point within the distance threshold D_{max} of the Cartesian plane is the distance covered within the LoS communication link. In Figure 2, the conceptual UE trajectory diagram within a Cartesian plane that shows the UE probable mobility pattern with respect to the placement of the UEs for LoS communication is presented. The equation governing the UE placement with respect to the obstacle–free coefficient is given as thus:

$$dy.UE_i = \frac{Y_f - Y_{in}}{X_f - X_{in}} dx.UE_i + C_{x=0}.UE_i \quad (12)$$

Also, the UE's positional placement along a given linear path is expressed in Cartesian form as:

$$dx.UE_i = \left[\frac{\left(dy.UE_i - C_{x=0}.UE_i\right)}{(Y_f - Y_{in})}\right](X_f - X_{in}) \quad (13)$$

Figure 3 illustrates the scenario whereby the $C_{x=-1}$ exponent acts as an obstacle coefficient that indicates the UE mobility pattern to be outside the set threshold distance, which is assumed to be the Distance of the footprint (D_{fp}). Thus, with the pre– sence of the $C_{x=-1}$ exponent, a UE outside the D_{max} would still maintain communication link with a base station within the D_{fp}. This scenario depicts an NLoS communication link. Additionally, it is assumed that a UE movement from an initial

ISSN 1584 – 2665 (printed version); ISSN 2601 – 2332 (online); ISSN-L 1584 – 2665

point to any point outside the D_{max} but within the D_{fp} of the Cartesian plane is the distance covered within the NLoS communication link.

Similarly, to obtain the UE position at any instant along the Cartesian coordinate with respect to the obstacle–based coefficient ($C_{x=-1}$), Eq. (12) is re–written as Eq. (14) as:

$$d'y.\,UE'_i = \frac{Y'_f - Y'_{in}}{X'_f - X'_{in}}\,d'x.\,UE'_i + C_{x=-1}.\,UE'_i \qquad (14)$$

Thus, the positional placement of the UE for the obstacle–based coefficient is governed by the equation:

$$d'x.\,UE_i{}' = \left[\frac{(d'y.\,UE'_i - C_{x=-1}.\,UE'_i)}{(Y'_f - Y'_{in})}\right](X'_f - X'_{in}) \qquad (15)$$

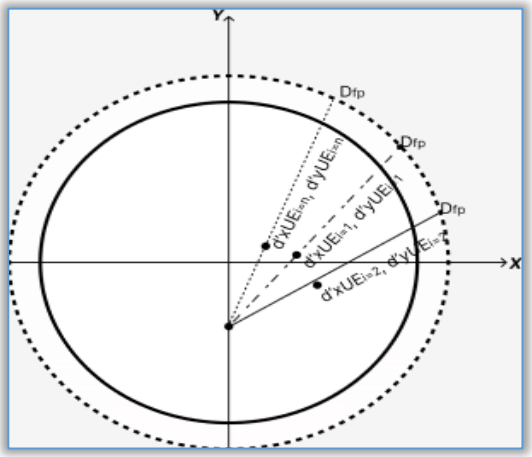

Figure 3: UE Placement Trajectory for Obstacle–based Scenario

where:

dx is the instantaneous position of the UE along the x–axis during placement.

UE_i represent a finite number of UE ($i = 1 \ldots \ldots N$).

dy defines the instantaneous position of the UE along the y–axis during placement.

$C_{x=0}$ denotes the obstacle–free coefficient.

Y_f is the final position of the UE along the y–axis.

Y_{in} represent the initial position of the UE along the y–axis.

X_f defines the final position of the UE along the x–axis.

X_{in} is the initial position of the UE along the x–axis.

Formulating the Handover Triggering Conditions

Based on event A3 as adopted in this study, when a neighbor base station becomes offset better than the serving base station, the trigger condition [24] is expressed as:

$$HO_{triggering} = \begin{cases} 1 \text{ if } RSRP_n^k \geq RSRP_n^j + offset \\ 0 \qquad \text{otherwise} \end{cases} \qquad (16)$$

where, $RSRP_n^k$ and $RSRP_n^j$ are the Reference Signal Received Power of the target base station k and serving base station j. Offset represents the handover margin.

The user defined condition for handover triggering is given in Eq. (17):

$$\gamma = \begin{cases} 1 & \left[\gamma_n^j(t_o) < \gamma_n^{min}\right], \left[\gamma_n^k(t) \geq \gamma_n^j(t) + offset\right], \left[\gamma_n^{max} - \gamma_n^{min} > t\right] \\ 0 & \text{otherwise} \end{cases} \qquad (17)$$

A threshold value of $1Tbit/sec$ was selected based in the simulation analysis from the work of [16]. Thus, the improved model equation for handover triggering is now given as:

$$\gamma^* = \begin{cases} 1 & \left[\gamma_n^j(t_o) < \gamma_n^{min}\right], \left[\gamma_n^k(t) \geq \gamma_n^j(t) + offset\right], \left[\gamma_n^{max} - \gamma_n^{min} > t\right], R_{i,j} \\ 0 & \text{otherwise} \end{cases} \qquad (18)$$

where $R_{i,j} \leq 1Tbit/sec$

However, in order to minimize handover, the volume of the transmitted data with respect to time is computed [16] using Eq. (19):

$$R_n^k(t) = \int_t^{t_n^k} r_n^k(t)dt \qquad (19)$$

Where $R_n^k(t)$ is the overall transmitted data from time t to $t_n^k$when UE switches to base station k $r_n^k(t)$ is the expended data with respect to time.

The system throughput is an added metric that was considered in ensuring an efficient handover process for effective system performance. The threshold value used in this study was gotten from the system throughput analysis as given in the work of [16]. The throughput condition is given as:

$$T_{HO} = \begin{cases} 1 & T < 1Tbits/sec \\ 0 & T \geq 1Tbits/sec \end{cases} \qquad (20)$$

Thus, for handover to occur in the improved model, the following conditions are needed:

ISSN 1584 – 2665 (printed version); ISSN 2601 – 2332 (online); ISSN-L 1584 – 2665

$$\gamma^{*} = \begin{cases} 1 & [T < 1\text{Tbits/sec}] \ \left[\gamma_n^j(t_o) < \gamma_n^{min}\right], \left[\gamma_n^k(t) \geq \gamma_n^j(t) + \text{offset}\right], [\gamma_n^{max} - \gamma_n^{min} > t] \\ 0 & \text{otherwise} \end{cases} \quad (21)$$

$$\gamma^{**} = \begin{cases} 0 & [T \geq 1\text{Tbits/sec}] \ \left[\gamma_n^j(t_o) < \gamma_n^{min}\right], \left[\gamma_n^k(t) \geq \gamma_n^j(t) + \text{offset}\right], [\gamma_n^{max} - \gamma_n^{min} > t] \\ 1 & \text{otherwise} \end{cases} \quad (22)$$

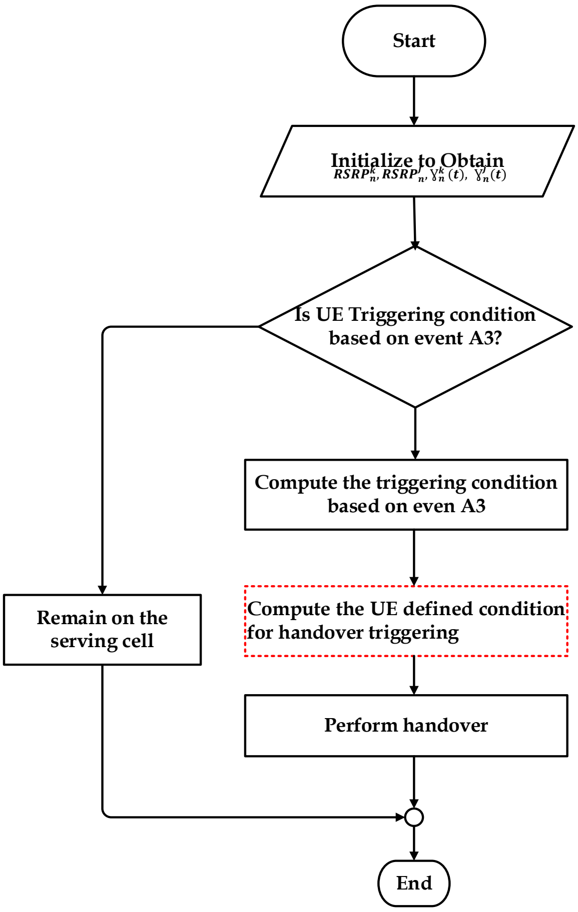

Figure 4: Flowchart of the Improved Handover Triggering Model

where γ^{*} defines the improved handover triggering condition for $T < 1\text{Tbits/sec}$ and γ^{**} denotes the improved handover triggering condition for $T \geq 1\text{Tbits/sec}$.

Figure 5 presents the simulated mobility pattern of the users across the femtocells, picocells and macrocell base stations.

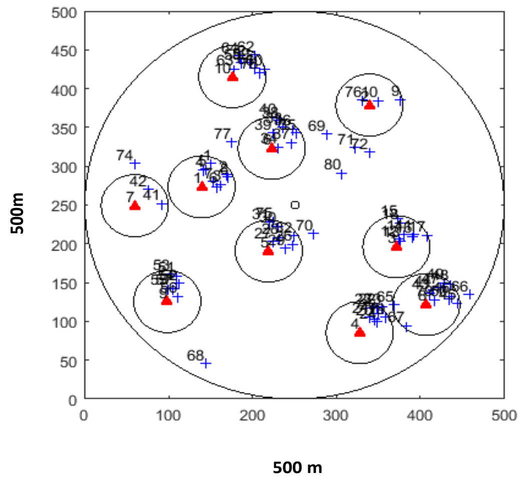

Figure 5: Snippet of the Simulated User Mobility Pattern

In this paper, the red triangles represent the femtocells, whilst the medium and large circles indicate the picocells and macrocell, respectively. Also, the numbers as seen inside the circles describes the simulated number of users in each cell at any point in time. A coverage size of 500m by 500m was assumed in this study. This is so selected in order to effectively cater for the earlier assumed distance coverage of this research paper that was defined for both LoS and NLoS users.

5. SIMULATION SET–UP

The developed CPH scheme is simulated with MATLAB R2018a. The simulation's standard parameters, which align with the simulation scenario employed in a system–level simulator for 5G mobile networks [16], are displayed in Table 1.

Table 1. Simulation parameters [16]

S/N	Parameter	Values
1	Maximum coverage length of LoS Path	200m
2	Macro BS bandwidth	20MHz
3	Macro BS frequency	2GHz
4	mm–Wave BS bandwidth	5GHz
5	mm–Wave BS frequency	38GHz
6	Macro BS transmit power	20W
7	Pico BS transmit power	1W
8	Femto BS transmit power	0.1W
9	Velocity of UE	2.7m/s, 10m/s
10	Minimum UE data rate	1Gbps
11	End–to–end latency	10ms
12	Antenna gain	10dB
13	Antenna transmit power	30dB
14	Interference power density	0.5dBm/Hz
15	Noise power density	–174dBm/Hz
16	Reference signal Received power	–80dBm

6. RESULT DISCUSSION

In this study, the number of handover and average throughput at varying number of femto–BS are metrics used to analyze the network performance and efficiency. The data obtained are graphically represented in Figure 6 and Figure 7 respectively.

7. CONCLUSION

The CPH scheme in terms of number of Femto Base Station (FBS) obtained an average number of 4.15×10^4 handovers when compared to the RBH scheme which obtained 9.02×10^4 handovers and the Seamless Handover Technique (SMART) scheme that obtained 4.46×10^4handover. This corresponds to 53.98% and 6.87% handover percentage reduction, respectively.

Furthermore, the CPH scheme in terms of number of FBS obtained an average throughput value of 3.02×10^{12} bits when compared to the RBH scheme which obtained 2.75×10^{12} bits and the SMART scheme that obtained 2.79×10^{12} bits. This translates to 9.39% and 9.15% average throughput percentage improvement, respectively. By implication, the user experience and network performance were improved upon especially leveraging on the merits of the conceptualized Cartesian coordinates.

References

[1] Li, J., Niu, Y., Wu, H., Ai, B., Chen, S., Feng, Z., and Wang, N., "Mobility support for millimeter wave communications: Opportunities and challenges," IEEE Communications Surveys & Tutorials, 24(3), 1816–1842, 2022.

[2] Mihovska, A., and R. Prasad, "Spectrum sharing and dynamic spectrum management techniques in 5G and beyond networks: A survey," Journal of Mobile Multimedia, 65–78. 2021.

[3] Al–Achhab, T., Abboud, F., and Assalem, A., "A Robust Self–Optimization Algorithm Based on Idiosyncratic Adaptation of Handover Parameters for Mobility Management in LTE–A Heterogeneous Networks," IEEE Access, 9, 154237–154264. 2021.

[4] Arshad, R., El Sawy, H., Sorour, S., Al–Naffouri, T. Y., and Alouini, M. S., "Velocity–aware handover management in two–tier cellular networks," IEEE Transactions on Wireless Communications, 16(3), 1851–1867. 2017.

[5] El Banna, R., El Attar, H. M., and Abou El–Dahab, M. M., "Fast adaptive handover using fuzzy logic for 5G communications on high–speed trains," Proceedings of 16th IEEE International Conference on Telecommunications (ConTEL) pp. 10–17, 2021.

[6] Kishida, A., Morihiro, Y., Asai, T., and Okumura, Y., "Cell selection scheme for handover reduction based on moving direction and velocity of UEs for 5G multi–layered radio access networks," Proceedings of International Conference on Information Networking (ICOIN) 10(3), 362–367, 2018.

[7] Koda, Y., K. Nakashima, Yamamoto, K., Nishio, T., and Morikura, M., "Handover management for mmWave networks with proactive performance prediction using camera images and deep reinforcement learning," IEEE Transactions on Cognitive Communications and Networking, 6(2), 802–816, 2019.

[8] Kurgalin, S., and Borzunov, S., Algebra and Geometry with Python: Springer Cham, pp. 277–305, 2021.

[9] Mollel, M., Ozturk, M., Kisangiri, M., Kaijage, S., Onireti, O., Imran, M. A., and Abbasi, Q. H., "Handover management in dense networks with coverage prediction from sparse networks," Proceedings of IEEE Wireless Communications and Networking Conference Workshop (WCNCW) 17(9), 1–6. 2019.

[10] Mollel, M. S., Abubakar, A. I., Ozturk, M., Kaijage, S., Kisangiri, M., Zoha, A., and Abbasi, Q. H., "Intelligent handover decision scheme using double deep reinforcement learning," Physical Communication, 42, 101133, 2020.

[11] Njoku, F. C., Ibikunle, F., and Adikpe, A.O., "A Review on Discontinuous Reception Mechanism as a Power Saving Approach for 5G User Equipment at Millimeter–Wave Frequencies," Proceedings of IEEE International Conference on Science, Engineering and Business for Sustainable Development Goals (SEB–SDG) (Vol. 1), pp. 1–7, 2023.

[12] Njoku, C. F., Tekanyi, A. M. S., and Babatunde, M. O., "An Efficient Technique in the Minimization of Unnecessary Handover for Macro–Femto Cells in LTE Network," Arid Zone Journal of Engineering, Technology and Environment, 14(4), 604–613, 2018.

[13] Qi, K., Liu, T., and Yang, C., "Federated learning based proactive handover in millimeter–wave vehicular networks," Proceedings of 15th IEEE International Conference on Signal Processing (ICSP) 42(1), 401–406, (2021).

[14] Sarkar, S., and Ghosh, S. C., "Mobility Aware Path Selection for Millimeter–Wave 5G Networks in the Presence of Obstacles," Proceedings of International Conference on Computer and Communication Engineering, 11(3), pp. 67–80, 2023.

[15] Shayea, I., Ergen, M., Azizan, A., Ismail, M., and Daradkeh, Y. I., "Individualistic dynamic handover parameter self–optimization algorithm for 5G networks based on automatic weight function," IEEE Access, 8, 214392–214412, 2020.

[16] Sun, Y., Feng, G., Qin, S., Liang, Y. C., and Yum, T. S. P., "The SMART handoff policy for millimeter wave heterogeneous cellular networks. IEEE Transactions on Mobile Computing," 17(6), 1456–1468, 2017.

[17] Tahir, S., "A novel architecture for 5G ultra dense heterogeneous cellular network," International Journal of Advanced Computer Science and Applications, 9(11). 2018.

[18] Wang, C. X., Haider, F., Gao, X., You, X. H., Yang, Y., Yuan, D., and Hepsaydir, E., "Cellular architecture and key technologies for 5G wireless communication networks," IEEE communications magazine, 52(2), 122–130, 2014.

[19] Wang, H., and Li, B., "Double-deep Q-learning-based handover management in mmWave heterogeneous networks with dual connectivity," Transactions on Emerging Telecommunications Technologies, 35(1), 4907, 2024.

[20] Yu, J., Zhang, and Chen, Y., "Joint optimization of access delay and handover latency in 5G satellite–terrestrial integrated networks," IEEE Transactions on Vehicular Technology, 70(1), 464–476, 2021.

[21] Zhang, Z., Jiang, Z., Yang, B., She, X., "A Beamforming–Based Enhanced Handover Scheme with Adaptive Threshold for 5G Heterogeneous Networks," Electronics, 12(19), 4131, (2023).

[22] Zhu, H., and Peng, Y. I., "Research on adaptive handover scheme based on improved genetic algorithm," Procedia Computer Science, 166, 557–562, 2020.
[23] 3GPP, "Technical Specification Group Radio Access Network; Evolved Universal Terrestrial Radio Access (E–UTRA) and Evolved Universal Terrestrial Radio Access Network (E–UTRAN); Overall Description; Stage 2," Technical Report, 3GPP TS 36.300 Version 12.5.0, Release 12, 2014.
[24] 3GPP, "Technical Specification Group Radio Access Network; Solutions for NR to Support Non–Terrestrial Networks (NTN)," 3GPP TR 38.821 Release 15, 2019.
[25] Silva, K. D. C., Becvar, Z., and Frances, C. R. L., "Adaptive hysteresis margin based on fuzzy logic for handover in mobile networks with dense small cells," IEEE Access, 6, 17178–17189, 2018.
[26] Okpeh, A. A, Tekanyi, A. M. S., Yaro, A. S., and Okpe, J. M., "Multicriteria and Quality of Service–Aware Vertical Handover Solution for V2I–Communication in Multitier Heterogeneous Networks," Jordan Journal of Electrical Engineering, 10(3), 383–396, 2024.
[27] Okpeh, A. A., Okpe, J. M., Tekanyi, A. M. S., and, Tanko, N. A., "Cooperative Multicriteria Handover Management for Reliable V2I Communication and Improved QoS in Overlayed Heterogeneous Network Environment," ANNALS of Faculty Engineering Hunedoara–International Journal Of Engineering, 4(21), 115–124, 2023.

ISSN 1584 – 2665 (printed version); ISSN 2601 – 2332 (online); ISSN-L 1584 – 2665